African Journal of Advanced Pure and Applied Sciences (AJAPAS)

Online ISSN: 2957-644X

Volume 3, Issue 1, January-March 2024, Page No: 235-242

Website: *https://aaasjournals.com/index.php/ajapas/index*

معامل التأثير العربي 2023: (1.55) **SJIFactor 2023: 5.689** **ISI 2022-2023: 0.557**

Effect of the Thermomechanical Treatment on Corrosion Resistance of API 5L X70 Pipeline Steel

Mohamed M. Salem [1*], Hesham Mraied [2], Adel M. Burakhis [3], Ibrahim K. Husain [4]

[1, 4] The Advanced Center of Technology, Tripoli, Libya

[2] Department of Materials and Metallurgical Engineering, University of Tripoli, Tripoli, Libya

[3] The Nuclear Research Centre, Tripoli, Libya

[*]Corresponding author: mmohelby@gmail.com

Received: December 28, 2023	Accepted: February 23, 2024	Published: March 24, 2024

Abstract

The final microstructure and subsequent properties of state of the art HSLA pipeline steel plates are highly dependent on both the controlled rolling conditions and accelerated cooling conditions. This work utilized a novel physical deformation simulator to evaluate the evolution of microstructure in an API 5L X-70 steel during finish hot deformation and cooling. A series of plane strain compression (PSC) tests have been conducted to simulate the processes of plate rolling. The corrosion behaviour of received samples processed by TMCP was examined by potentiodynamic polarisation and electrochemical impedance spectroscopy tests. Electrochemical tests show corrosion resistance improvement due to microstructure refinement in selected TMCP process parameters.

Keywords: High strength low alloy steel HSLA Steel, Plane Strain Compression Test PSC, Electrochemical Impedance Spectroscopy EIS, Potentiodynamic, Thermomechanical Controlled Processing TMCP.

Cite this article as: M. M. Salem, H. Elmaried, A. M. Burakhis, I. K. Husain, "Effect of the Thermomechanical Treatment on Corrosion Resistance of API 5L X70 Pipeline Steel," *African Journal of Advanced Pure and Applied Sciences (AJAPAS)*, vol. 3, no. 1, pp. 235–242, January-March 2024.

تأثير المعالجة الثيرموميكانيكية على مقاومة التآكل لفولاذ خطوط الأنابيب API 5L X70

محمد مفتاح سالم[1*]، هشام يوسف المريض[2]، عادل مصطفى بورخيص[3]، ابراهيم خليفة حسين[4]

[4،1] المركز الليبي المتقدم للتقنية - طرابلس، ليبيا

[2] قسم هندسة المواد والمعادن، جامعة طرابلس، طرابلس، ليبيا

[3] مركز البحوث النووية - تاجوراء، ليبيا

الملخص:

أظهرت الدراسات أن البنية المجهرية والخواص الاخرى لصفائح الصلب عالي الجهد منخفض السبائك HSLA تعتمد بشكل كبير على كل من ظروف الدرفلة التي يتحكم فيها وظروف معدلات التبريد. في هذا البحث تم استخدام محاكي تشكيل لتقييم البنية المجهرية للصلب API 5L X-70 اثناء التشكيل على الساخن مع التحكم في التبريد. تم إجراء سلسلة من الاختبارات على عينات ضغط الانفعال المستوي (PSC) لمحاكاة درفلة الصفائح. سلوك التآكل للعينات التي جهزت باستخدام TMCP، وتم اختبارها عن طريق الاستقطاب الديناميكي واختبار التحليل الطيفي للمقاومة الكهروكيميائية. الاختبارات الكهروكيميائية أظهرت تحسنًا في مقاومة التآكل نتيجة لتقليل حجم الحبيبات لبعض عمليات TMCP.

الكلمات المفتاحية: فولاذ عالي القوة ومنخفض السبائك (HSLA)، اختبار ضغط إجهاد المستوى (PSC)، التحليل الطيفي للمقاومة الكهروكيميائية (EIS)، المعالجة الحرارية الميكانيكية (TMCP).

1. Introduction

Oil and natural gas are considered the main sources of energy in the world and the demand and consumption of their products are growing constantly. The materials used in building equipment for the oil and gas industry must meet the safety requirement for production and transportation of these products. The materials used must respond satisfactorily to the harsh conditions of the petroleum extraction and subsequent transportation. Some important properties are high mechanical strength, fracture toughness, weldability and resistances to corrosion and hydrogen induced damages in acidic environments

HSLA steels, known also as low micro-alloyed steels are those designed to provide superior mechanical properties and resistance to atmospheric corrosion when compared to other steels with the same chemical composition. The required mechanical properties are achieved by controlling the addition of alloying elements and severe production procedure. HSLA steels are classified into different categories; one of these is API x70, which has replaced the API 5L X65 (the highest grade approved for sour gas applications) in pipelines production for the oil and gas industry.

HSLA steel has good properties, such as strength (over 275 MPa or 40 ksi), toughness, formability, weldability, and corrosion resistance. These mechanical properties are obtained by special processing techniques and alloying elements. The alloying elements are as follows: Carbon typically between 0.02 and 0.04% up to ~0.2%, Manganese content up to 2.0%, Nickel and Chromium and Copper and Molybdenum are limited to less than 1.5%, Silicon up to ~0.5%, Niobium ~0.02%, and Small quantities of nitrogen, vanadium, titanium, and zirconium are used in various combinations [1]

HSLA steel is used in different industries such as in oil and gas conveying pipelines and storage tanks, heavy-duty highway and off-road vehicles including mine and railroad cars, in constructions such as Bridges, offshore structures, power transmission towers, light poles, and building beams and panels, in addition to barges and dredges, snowmobiles, lawn mowers, and passenger car components[1].

HSLA steels including API x70 are produced by TMCP to obtain superior mechanical properties, which allows for the manufacturing of pipelines with thinner walls, leading to relevant savings.

As the mechanical performance of low carbon steel is largely determined by the ferrite grain size, whereas finer grain sizes are favorable for mechanical properties. However, due to the higher energy and chemical activity of grain boundaries, a high density of these boundaries might increase the reactivity of the surface through increased electron activity and diffusion, and hence, it can affect corrosion resistance. Higher corrosion resistance performance results in longer service of the steel structures. Therefore, studying the effect of grain size on the corrosion resistance of low carbon steel is an important subject. [2]

Oil pipelines carry different fluids including hydrocarbons, water, gases and other miscellaneous substances which could deteriorate the internal surface of the pipeline. Whereas the external surface of the pipeline is subjected to atmospheric corrosion as well as to corrosive species (Cl^-) related to the marine environment. In general corrosion in the oil and gas industry can take different forms including (sweet corrosion) due to carbon dioxide, (sour corrosion) due to hydrogen sulphide and corrosion by oxygen in water injection [3]. The marine environment is extremely abundant and corrosive with very high salt concentrations mainly chloride ions. This will lead to severe corrosion attacks to the metal used in the structures and in the transport system of the oil and gas industries [4]. Bacterial attachment and subsequent biofilm formation on material surfaces can influence the deterioration by changing the physical or chemical properties of steel structures. In the biofilm may co-exist several microbial species, whose activity can result in the production of enzymes, EPS, organic and inorganic acids, which in turn may affect the cathodic and/or anodic reactions on metals, increasing the speed of electrochemical processes in biofilm/metal interface [5].

The objective of this work is to experimentally investigate the corrosion behavior of API 5L x70 pipeline steel produced using different thermomechanical processing routes. Variations in processing parameters will be applied with the intention of changing the structure of pipeline steels used for this study.

2. Experimental Procedure

2.1 Samples Preparation:

Four groups of specimens each contain three samples (the groups will be referred to as AS-R, A2, A6, and A15). The chemical composition of the API 5L X-70 HSLA steel is listed in Table 1, and the TMPC parameters for the processed specimens are shown in Table 2.

Table 1. The chemical composition (wt. %) of X-70

C	Si	Mn	P	S	N	Nb	Ni	Cr	Al
0.097	0.31	1.44	0.01	0.001	0.0052	0.057	0.06	0.03	0.045

Table 2. TMCP Deformation schedules of API 5L X-70 specimens

Sample	Manufacturing Process	Deformation Temperature (°C)	Deformation (%)	Cooling rate
AS-R	TMP			
A2	TMCP	950	55%	6°C/Sec.
A4	TMCP	850	40%	6°C/Sec.
A6	TMCP	950	60%	6°C/Sec.
A15	TMCP	850	60%	6°C/Sec.

AS-R (As received) samples are used as control samples. A2, A6, and A15 were subjected to a series of plane strain compression tests to simulate TMCP plate rolling under the influence of finishing temperature, cooling rate, and pass reduction. TMCP tests were carried out using a servo-hydraulic thermomechanical compression (TMC) machine [6]. During TMCP, all samples were reheated to 1200 °C, held for 60 seconds, and then cooled down to a specific deformation temperature (950 °C for A2 and A6, and 850 °C for A15). Soon after reaching the deformation temperature, samples were subjected to compression to a true strain of 0.4 (2 passes) for A2, and 3 passes for A6 and A15. The cooling rate for all three specimen groups was (6 °C/s), as illustrated schematically in Figure 1.

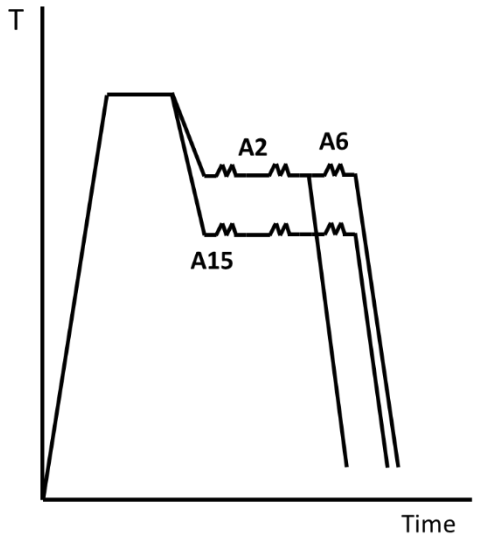

Figure 1. Schematic illustration of TMCP processes.

All specimens were cut to the same dimensions of 1.35 cm by 0.7 cm, yielding a surface area of ~ 0.95 cm². A copper wire was soldered to one face of the square piece. This face, including the contact, and the edges of the samples were covered with two-part epoxy resin and dried at room temperature for at least 24 hours, leaving just one face (`0.95 cm²) exposed. The samples in Figures 2.a and b were then mechanically polished with a set of SiC papers down to 1200 grit.

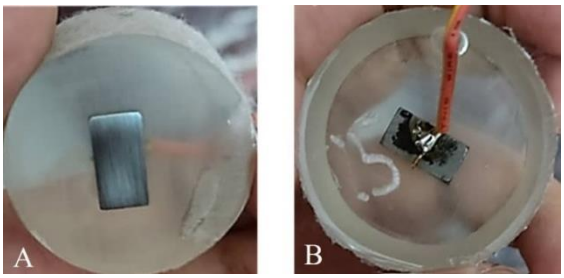

Figure .خطأ! لا يوجد نص من النمط المعين في المستند **.** HSLA sample for electrochemical tests

2.2 Electrochemical Tests

All electrochemical measurements were performed at room temperature using a Gamry Reference 600® Potentiostat, with the conventional three-electrode cell Figure 3 composed of the sample, graphite rod, and a commercial saturated calomel electrode (saturated KCl internal solution) as the working, counter, and reference electrode, respectively. The electrolyte was stagnant and aerated in a 3.5 wt. % NaCl solution, simulating a marine environment.

The Open circuit potential measurements were conducted regularly over a period of 100 hours. Electrochemical impedance spectroscopy (EIS) tests were conducted after 24 hours of immersion in the electrolyte at EOC in the frequency range of 10 kHz to 100 MHz, 5 points per decade, and 10 mV rms sinusoidal potential excitation. Potentiodynamic polarisation (PD) measurements were conducted at a constant scan rate of 0.167 mV/s, starting from the open circuit potential (EOC) to a cathodic potential (-300 mV to EOC) up to an anodic potential (~ +300 mV vs EOC). The obtained data was then fitted using Gamry E-chemanalytic software. All electrochemical tests were conducted at room temperature, and to ensure data reproducibility and accuracy, the results of a minimum of three samples are reported for each electrochemical test.

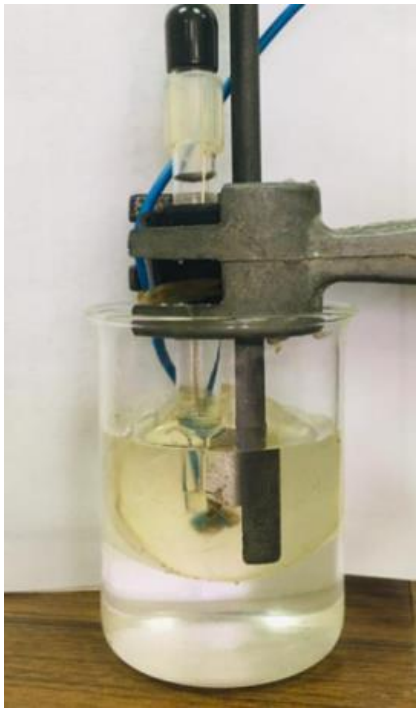

Figure 3. Setup for electrochemical tests.

3. Results and Discussion

3.1 Open Circuit Potential

For the long-term test, Figure 4. Shows that the Eoc of all samples was ~ −600 mVSCE upon immersion in a 3.5 wt. % NaCl solution. Eco was then shifted towards more negative values as exposure time increased and reached to ~ −700 mVSCE at 20 hours. Afterwards, EOC stabilized at ~ −750 mVSCE for all samples. These values are in good agreement with those recorded for HSLA steels in the same environment [7]. The evolution of Eoc indicated that the TMCP process and subsequent microstructure refinement had no effect on the Eoc as well as the stable local Passivity breakdown upon exposure to this environment [8, 9].

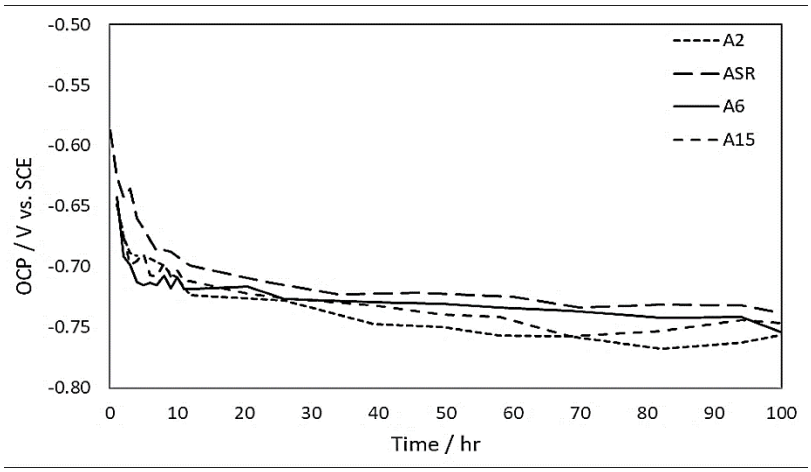

Figure 4. Long term evolution of Eoc samples immersed in 3.5 wt. % NaCl solution.

3.2 Electrochemical Impedance Spectroscopy

To evaluate the corrosion mechanisms of the samples, EIS measurements were conducted after EOC stabilisation for 24 hours in a 3.5 wt. % NaCl solution. The Nyquist diagram for representative results is shown in Figure 5., The diagrams of

all tests were generally similar in having a single capacitive loop shape, comparable with what could be expected from a polarisation resistance resulting from Faradaic processes, coupled with an interfacial charge storage process.

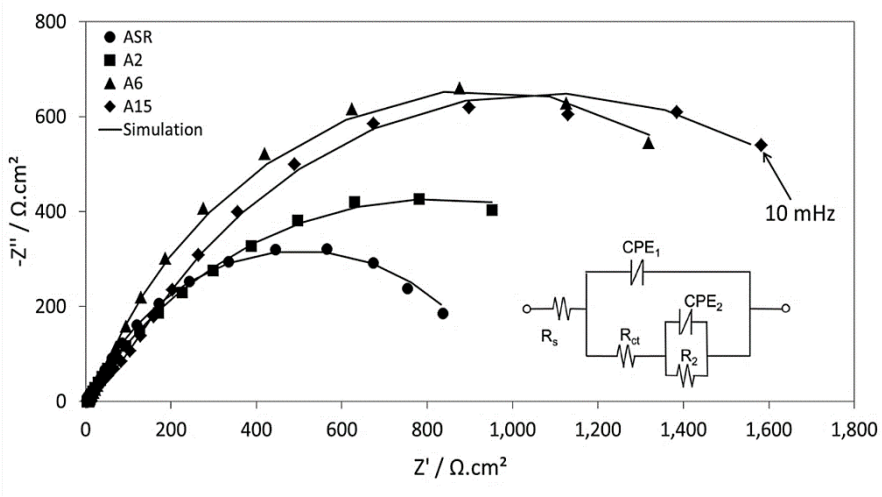

Figure 5 Representative Nyquist plots (scattered data) of samples EOC stabilization for 24 hours in the electrolyte.

The experimental data were interpreted using the analogue equivalent circuit model shown as an inset in Figure 5. A constant phase element (CPE) was used instead of a capacitor due to the expected depression of the Nyquist curve at low frequencies. Rs represents the ohmic solution resistance. In its simplest form, the solution-metal interface includes a polarisation resistance (RP) and a CPE. The Nyquist results showed similar corrosion mechanisms for four samples but a larger capacitive loop for TMCP-treated samples (A2, A6, and A15). The impedance of the non-ideal capacitance CPE is represented as:

$$Z_{CPE} = Y_o^{-1}(j\omega)^{-n} \quad (3.1)$$

Where Yo is a constant, j = (-1)1/2, ω is the angular frequency, and n is a real number between 0 and 1. The polarisation resistance (RP) for A2, A6, and A15 is (1790± 300) Ω.cm2, (1980± 100) Ω.cm2, and (2200 ± 300) Ω.cm2, respectively. These values are significantly larger than the value obtained for AS-R (974 ± 800) Ω.cm2) indicating the enhanced resistance to the flow of current through the metal surface as a result of grain refinement during TMCP processes. The corrosion current density (icorr) from EIS tests was estimated from the RP using the Stern-Geary equation:

$$i_{corr} = B/R_P \quad (3.2)$$

Where B is the apparent Stern-Geary coefficient and can be estimated from:

$$B = \frac{\beta_a . \beta_c}{2.3(\beta_a + \beta_c)} \quad (3.3)$$

Where βa and βc are the anodic and cathodic Tafel slopes, respectively, typically measured from cyclic potentiodynamic polarisation experiments. In this work, the value of B was chosen to be equal to 0.026 V. icorr was converted to corrosion rate (C.R) in micrometres per year as shown in Figure 6. Using Faraday's conversion (C.R (um/y) = icorr (A/cm2) x 1.16x10+6).

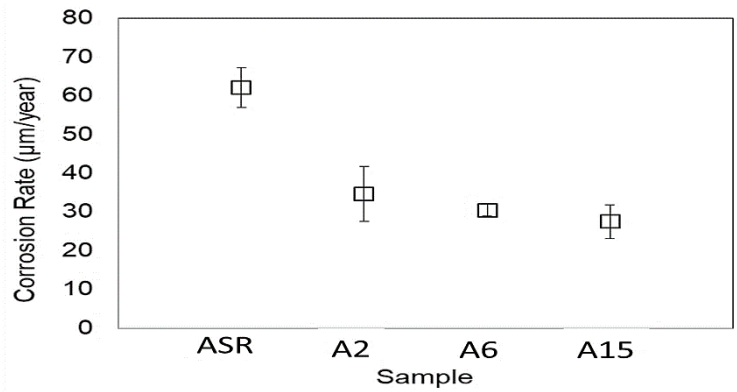

Figure 6 Corrosion rates in (µm/year) of AS-R, A2, A6 and A15 after 24 hr immersion in 3.5 wt% NaCl solution estimated from EIS tests.

As shown in figure 6, the corrosion rate for A2, A6, and A15 is (34 ± 7) µm /year, (30 ± 1.5) µm /year, and (28 ± 4) µm /year, respectively. These values are significantly larger than the value obtained for AS-R (62 ± 5) µm /year, indicating enhanced corrosion resistance (~ by half) as a result of the evolved microstructure changes during TMCP processes.

3.3 Potentiodynamic Polarization tests

Figure 7. Shows representative cyclic polarisation curves of four samples after 24 hours of immersion in a 3.5 wt% NaCl solution. The values of crossover potentials of zero current (Ezero current) of AS-R are - 0.750VSCE. This value is similar to the values measured for A2, A6, and A15 (-0.730VSCE, -0.690VSCE and -0.730VSCE, respectively). Ezero current values agreed reasonably well with the values of Eoc observed during the long-term exposure tests and those values observed before initiating the scans. The anodic part of the PD curves of all samples indicated active dissolution upon entering the anodic current regime.

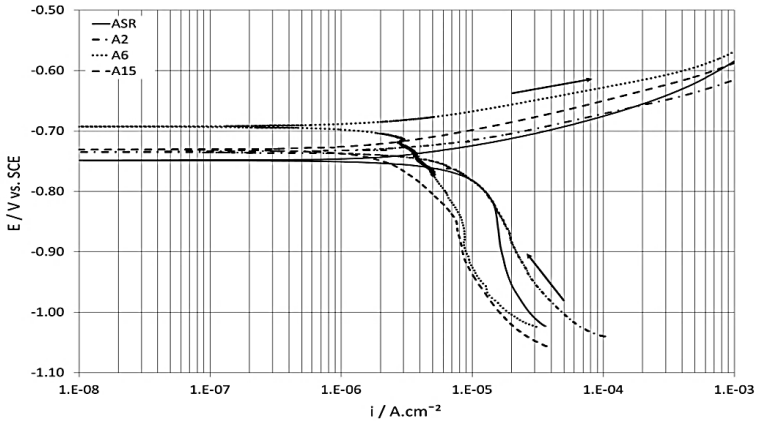

Figure 7. Typical potentiodynamic curves of AS-R, A2, A6, and A15 after 24 hr immersion in 3.5 wt% NaCl solution.

The corrosion rate in µm/year shown in Figure 8, was estimated by Faradic conversion of the icorr (1 µA/cm2 corresponds to approximately 22.6 µm/year). It was found that the corrosion rate of AS-R (150 ± 30 µm/year) is reduced significantly by the TMCP process. The corresponding values of A2, A6, and A15 samples are 70 ± 20, 30 ± 8 and 50 ± 5 µm/year, respectively.

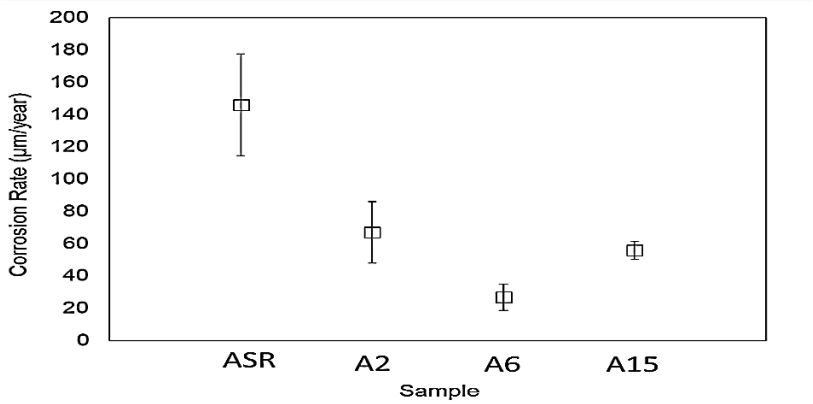

Figure 8. Corrosion rates in (um/year) of AS-R, A2, A6, and A15 after 24 hr immersion in 3.5 wt% NaCl solution estimated from Pd tests.

3.4 Grain size, hardness and corrosion rates

Figure 9. Shows the relationship between hardness and grain size (these data were obtained from the processed TMCP specimens, and the microstructure is shown in Figure 10. The inset figure shows the corrosion rate of all samples measured by both EIS and PD. It can be seen from Figure 3.6 that the TMCP process yielded a reduction in grain size and an enhancement in hardness. The enhancement in corrosion resistance of A2, A6, and A15 in this study could be related to the reduction in grain size achieved by TMCP processes. On the other hand, there was no linear relation between grain size and hardness values in Figure 9. The measured grain size showed the finer grain (TMCP-processed specimens) were achieved by enhanced hardness and an improvement in corrosion resistance when compared with AS-R specimens.

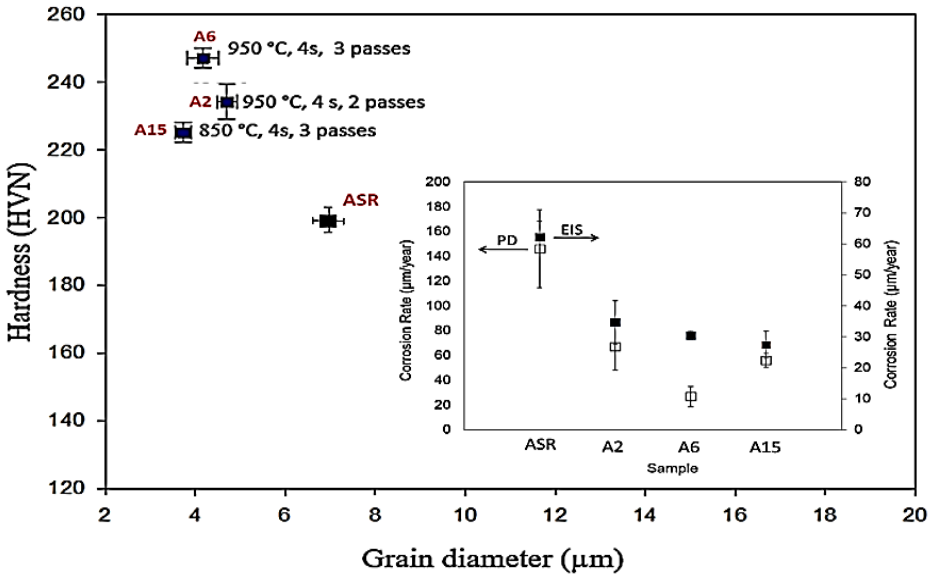

Figure 9. Correlation between grain size, hardness and corrosion rates.

3.5 Microstructure analysis

Figure 10. Shows the microstructural evolution under different deformation conditions. The following findings are made: The AS-received microstructure shows a mixture of polygonal ferrite and banded pearlite structures. Pearlite is a lamellar structure that consists of alternating layers of ferrite and cementite (Fe3C), each of which reacts differently to corrosive environments. However, these phases have the lowest corrosion resistance among all microstructures due to the high density of lattice defects, which promote corrosion. [10]

Due to the deformation process (TMCP) of X-70, the microstructure evolved and showed acicular ferrite and Bainite constituents in Figure 10 (A6, A15). The refinement of grain size has been formed in the microstructure (A6, A15), especially due to the control of cooling rate (6 °C/s), which is the main factor in controlling the microstructure and is beneficial in promoting corrosion resistance, as shown in Figure 8. [11]

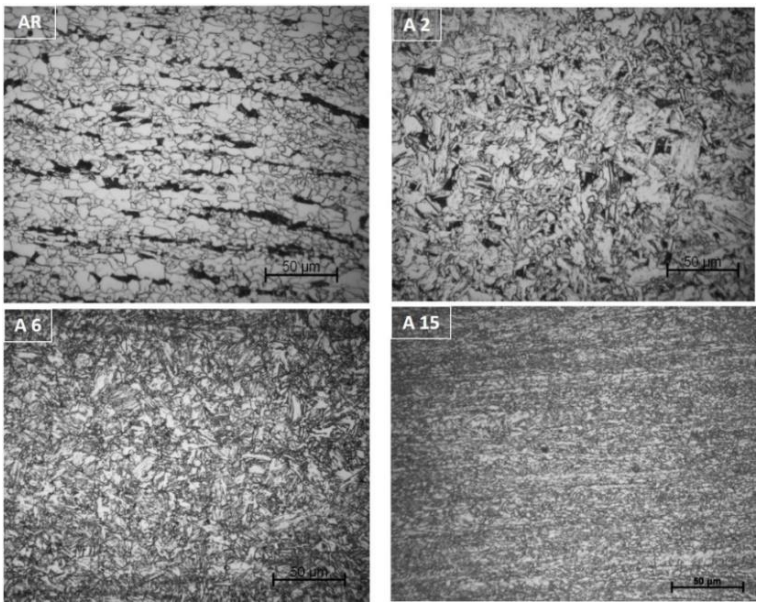

Figure 10 Optical micrographs of different TMCP conditions of API 5L X70.

Conclusions

The main purpose of this work is to experimentally investigate the corrosion behavior of the as-received API 5L x 70 pipeline steel produced using different thermomechanical processing routes. Variations in processing parameters were applied with the intention of changing the structure of the pipeline steels used for this study. It was found that the TMCP processes used led to a reduction in grain size and a corresponding enhancement in corrosion rates. The TMCP specimen processes showed more than 50% enhancement in the corrosion resistance compared with AS-R.

References

[1]. Sluiter, M.H.F., E. Pere Loma and D.V. Edmonds, Editors - First principles in modelling phase transformations in steels, in Phase Transformations in Steels, 2012, Woodhead Publishing. p. 365-404.

[2]. Klein, M., et al. Thermomechanically hot rolled high and ultra high strength steel grades-processing, properties and application. in Materials Science Forum. 2005. Trans Tech Publ.

[3]. Weglowski, M., et al., A comprehensive study on the microstructure and mechanical properties of arc girth welded joints of spiral welded high strength API X70 steel pipe. Archives of Civil and Mechanical Engineering, 2020. 20.

[4] Vera, R., F. Vinciguerra, and M. Bagnara, Comparative Study of the Behavior of API 5L-X65 Grade Steel and ASTM A53-B Grade Steel against Corrosion in Seawater. International Journal of Electrochemical Science, 2015. 10: p. 6187-6198.

[5]. Vitor Silva, L., L. Márcia Teresa Soares, and S. Eliana Flávia Camporese, Corrosion behavior of carbon steel API 5L X65 exposed to seawater. International Journal of Engineering and Technical Research, 2017. 7(10).

[6]. Yang, X., M. Salem, and E. Palmiere, The Effect of Processing Conditions and Cooling Rate on the Microstructure and Properties of API X-70 and API X-100 Steels. Materials and Manufacturing Processes, 2010. 25: p. 48-53.

[7]. Chen, L., D. Fu, and M. Chen, Modeling and mining dual-rate sampled data in corrosion potential online detection of low alloy steels in marine environment. Journal of Materials Science, 2020. 55(27): p. 13398-13413.

[8]. Mraied, H., W. Cai, and A.A. Sagüés, Corrosion resistance of Al and Al–Mn thin films. Thin Solid Films, 2016. 615: p. 391-401.

[9]. Escalera, D., et al., Effect of Nd 3+ Ion Concentration on the Corrosion Resistance of API X70 Steel in Chloride-Rich Environments. Advances in Materials Science and Engineering, 2018. 2018.

[10] S. Y. Shin, B. Hwang, S. Lee, N. J. Kim and S. S. Ahn, Correlation of microstructure and charpy impact properties in API X70 and X80 line-pipe steels (Materials Science and Engineering: A, 2007), 458(1-2), pp. 6281-289. 020021-5

[11] A. Qaban and S. Naher, "Influence of Al content on the corrosion resistance of micro-alloyed hot rolled steel as a function of grain size," in AIP Conference Proceedings (American Institute of Physics, 2018), 1960(1), pp. 040017.